Green Chemistry

Hydrophobic amine-based binary mixtures of active pharmaceutical and food grade ingredients: characterization and application in indium extraction from aqueous hydrochloric acid media

Journal:	*Green Chemistry*
Manuscript ID	GC-ART-07-2020-002452.R1
Article Type:	Paper
Date Submitted by the Author:	08-Sep-2020
Complete List of Authors:	Edgecomb, Joseph; Saint Martin's University, Natural Sciences Tereshatov, Evgeny; Texas A&M University College Station, Cyclotron Institute Zante, Guillaume ; University of Strasbourg; ADEME Boltoeva, Maria; University of Strasbourg Folden III, Charles; Texas A&M University College Station, Cyclotron Institute; Texas A&M University College Station, Department of Chemistry

ARTICLE

Hydrophobic amine-based binary mixtures of active pharmaceutical and food grade ingredients: characterization and application in indium extraction from aqueous hydrochloric acid media

Received 00th January 20xx,
Accepted 00th January 20xx

DOI: 10.1039/x0xx00000x

Joseph M. Edgecomb,[a,b] Evgeny E. Tereshatov,[a,*] Guillaume Zante,[c] Maria Boltoeva,[c] Charles M. Folden III[a,d]

The wide spread use of hazardous and expensive solvents for the liquid-liquid extraction (LLE) of critical metals has been a growing source of waste in the metal refinement industry. We have developed and characterized room temperature liquid hydrophobic binary mixtures based on common pharmaceutical and food grade compounds as sustainable, cost effective alternatives to both ionic liquids and conventional solvents. Additionally, we introduce liquid mixtures with Proton Sponge® (1,8-*bis*(dimethylamino)naphthalene), one of the strongest known organic bases. These mixtures have been applied to the LLE of indium(III) ions from hydrochloric acid solutions, displaying an extraction efficiency greater than 99% in some systems. A systematic approach to identifying the underlying mechanism of extraction, in particular relating to the charge, solubility, and complexation of the indium species in the organic phase has been developed.

Introduction

Twenty million metric tons of chemical waste are generated annually from the use of biohazardous solvents, particularly in fine chemical and pharmaceutical synthesis.[1] As a result, legislation in both the United States (Clean Air Act, 1991) and Europe (EU Solvents Emission Directive, 1999/13/EC) has been passed to address the negative environmental impacts of toxic waste production. Approaches for limiting the amount of toxic waste include both the reduction of solvent volume[2,3] and replacing conventional solvents with sustainable "green solvents".[4] The criteria for what constitutes a green solvent have become the subject of debate. Generally, a solvent is designated as green not only by its intrinsic properties (i.e. low toxicity, vapor pressure, etc.), but also by a sustainable method of production, such as biomass conversion.[5] Cost is also a significant consideration, as expensive green alternatives to conventional low cost solvents will have little impact on chemical processes in industry.

Two classes of solvents, ionic liquids and eutectic mixtures, have been established as green alternatives to traditional solvents. Ionic liquids are salts with a melting temperature bellow 100˚C, and generally consist of an organic cation and a broad range of potential anions.[2] Ionic liquids have been used in applications ranging from electrolyte solutions in electrochemistry[6] to liquid phase extraction of both organic[7] and metal[8,9] species. Eutectic solvents, sometimes considered to be a new generation of ionic liquids[10] are mixtures of at least two compounds combined in the composition corresponding the greatest melting point depression. Binary systems of certain compounds produce a glassy material where a melting point is not observed. Such systems are characterized by their glass transition temperature, a second-order phase transition. In this case, the low transition temperature mixtures (LTTMs) are discussed.[11,12] As opposed to ionic liquids, which contain discrete cations and anions, eutectics and LTTMs may be formed from various salts, metals and neutral organic compounds. Additionally, compounds with strong intermolecular hydrogen bonding may demonstrate lower than expected melting temperatures, forming a deep eutectic solvent (DES).[13,14] The same individual compounds can be used to form either ionic liquids or eutectics/LTTMs. The desired path way depends on the pK_a of compounds chosen; the eutectics/LTTMs will be synthesized if the hydrogen bond donor is weaker than the acid used to form the hydrogen bond acceptor.[11,15] Due to the broad range of starting materials available to form eutectic mixtures, these solvents have been tailored to specific applications in organo-catalysis,[2] metal processing,[16] and biodiesel synthesis.[17]

Recently, interest in hydrophobic ionic liquids has been driven in part by their capacity to extract metal species from aqueous solutions, in particular relating to the liquid-liquid extraction (LLE) of indium.[18-31] The use of indium, predominantly in electronic applications such as indium-tin oxide (ITO) and LCD's, has resulted in massive increase in global demand.[32] By contrast, the natural abundance of indium is low,[33] with more than half of the global supply coming from China according to both European[34] and United States[35] reporting agencies. As a

[a]*Cyclotron Institute, Texas A&M University, College Station, TX 77843 USA*
[b]*Department of Natural Sciences, Saint Martin's University, Lacey, WA 98503 USA*
[c]*Université de Strasbourg, CNRS, IPHC, UMR 7178, F-67000 Strasbourg, France*
[d]*Department of Chemistry, Texas A&M University, College Station, TX 77843 USA*
[*]*E-mail address of the corresponding author: etereshatov@tamu.edu*
Electronic Supplementary Information (ESI) available: [details of any supplementary information available should be included here]. See DOI: 10.1039/x0xx00000x

result, new techniques are needed in both the extraction of indium from zinc ore, as well as recycling indium from end of life electronics. A significant limitation to the application of eutectic mixtures and LTTMs to metal extraction is the relatively small number of hydrophobic eutectics that have been characterized in the literature. The majority of these solvents are used in the extraction of organic species.[36-40] Currently, to the best of our knowledge only a few studies[41-44] explore the extraction of metals, with just the former exploring indium extraction specifically. Therefore, much more study is needed into the applications of hydrophobic mixtures such as eutectics as cost effective and green alternatives to both conventional solvents and ionic liquids for the extraction of metals. To this end, non-ionic hydrophobic eutectics have been established as a new class of promising tunable solvents for metal extraction.[45]

The toxicity and biodegradability of eutectic solvents, as well as ionic liquids, are closely related to the properties of the starting material.[16] For example, it has been shown that other than a low vapor pressure, the environmental favorability of ionic liquids is not intrinsic, but rather dependent on composition.[46] Water immiscible compounds such as common pharmaceuticals and food grade ingredients are ideal potential candidates for sustainable LLE solvents. Also, systematic investigation of these solvents will be enhanced if initial compounds are inexpensive, commercially available and have a melting point below 100˚C. Similar screening criteria have been applied in several field applications of eutectic solvents. For example, many liquid-forming combinations of pharmaceutical compounds have been applied to organic extractions,[47] or to increase drug solubility in water and therefore enhance delivery.[48] However, these applications, generally dealing with hydrophilic solvents, are not suitable for LLE. Herein, we emphasize the applications of pharmaceuticals due the current use of indium as medical isotope (^{111}In) in biomedical imaging.

The goal of this paper is to identify and characterize novel applications of hydrophobic and low viscosity liquid binary mixtures based on active pharmaceutical and food grade ingredients with potential to serve as cost effective, green alternatives to ionic liquids and traditional solvents for indium liquid-liquid extraction from hydrochloric acid solutions.

Experimental

Chemicals. DL-menthol (hereafter abbreviated as Mnt, >98%, lot. 10200554) and methyl anthranilate (MA, >99%, lot. Q25E069) were purchased from Alfa Aesar. Lidocaine (Lid, 2-(diethylamino)-N-(2,6-dimethylphenyl)acetamide, MKCD6808) and proton sponge (PS, 1,8-Bis(dimethylamino)naphthalene, >99%, lot. BCBU7395) were purchased from Sigma Aldrich. Ibuprofen (Ibu, (4-isobutylphenyl)propanoic acid, >98%, lot BRIPC-BO) was purchased from TCL. All chemicals were used as ordered from the manufacture without further preparation. Deionized water was used from an ELGA PURELAB DV25 at 18.2 MΩ cm for preparation of all aqueous solutions. Aqueous HCl solutions were prepared from concentrated stock (Merk, 32%) and titrated with a Titroline 5000 automatic titrator (SI Analytics).

Preparation and characterization of Binary Mixtures. Binary mixtures were prepared in a one pot synthesis by combining varying mass ratios of each compound in 10% increments. The mixtures were melted in a water bath at approximately 20˚C higher than the highest melting point, mixed, and then left to equilibrate overnight before use. Mixtures were water pre-saturated through addition of 1 mass equivalent of water, thorough shaking, and left to equilibrate overnight. The water content of both water pre-saturated and dry solvents was measures with a Karl Fischer titrator (890 Titrando, Metrohm USA.) The dynamic viscosity was measured on a Brookfield LVT SN 16641 viscometer.

^{1}H Quantitative NMR. The solubility of the binary mixtures in the aqueous phase was measured by NMR (Bruker, 400 MHz). For all NMR measurements, deuterium chloride (Sigma Aldrich) and deuterium oxide (Sigma Aldrich) were substituted for HCl and water, respectively. An internal standard of maleic acid was added as a reference. Time constant (T1) analysis was conducted on all 5 compounds and the internal standard, with the later having the largest T1 of 5.4 ± 0.5 seconds. 30 seconds was used for D1 in all measurements in this report. The peaks chosen for quantification are outlined in Table S1 of the ESI, along with the observed T1 relaxation constants.

Table 1 Acidity of selected compounds at room temperature

Compound	Structure	pK_a	Ref.
Mnt	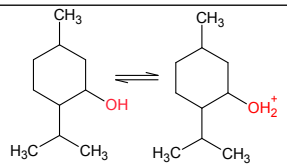	–0.81	49
MA	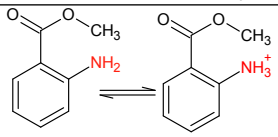	2.10	50,51
Ibu	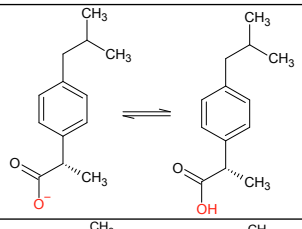	5.3	52
Lid	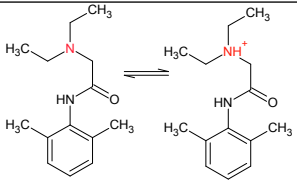	7.97	53,54

PS	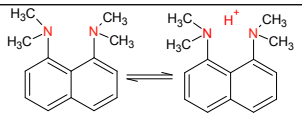	12.1	[55]

Table 2 Thermochemical properties of compounds used in this work

Compound	Melting Temperature (°C)	Ref.	Enthalpy of Fusion, Δh^{fus} (kJ/mol)	Ref.	Glass Transition Temperature (˚C)	Ref.
Mnt	30 ± 1 37	This work [39]	12 10	This work [57]	–54 ± 1	[56]
MA	21 ± 1 24	This work [58]	16	This work	–68.6 ± 0.5	This work
Ibu	73 ± 1 77	This work [59]	24 27	This work [60]	–46.5 ± 0.5 –45 ± 1	This work [61]
Lid	67 ± 1 68	This work [63]	15 16	This work [64]	–60 ± 2	[62]
PS	47 ± 1 48	This work [65]	17 20	This work [66]	Not observed	–

DSC Analysis. The mass ratio of compounds corresponding to the eutectic or LTTM composition for each binary system was determined with a differential scanning calorimeter (Q20 DSC, TA Instruments). Approximately 5 to 15 mg of sample was measured in an aluminum pan, with an empty pan serving as a reference. A scan speed of 5 ˚C min^{-1} was used over a temperature range of 40 ˚C to –90 ˚C, with subsequent heating back to 40 ˚C. Analysis was conducted with TA Universal Analysis software. All reported glass transition and melting values reflect the onset temperature.

Indium Extraction. Carrier-free ^{111}In [half-life 2.80 d, 171.3 keV (90.2%) and 245.5 keV (94.0%)] medical radioisotope (~15 mCi) was purchased from Mallinckrodt (St. Louis, Missouri, USA.) The production method is ^{112}Cd(p,2n)^{111}In, shipped in 0.05M HCl. A standard liquid-liquid extraction technique was followed with as-prepared (dry) or water pre-saturated (wet) binary systems. Equal volumes (0.5 mL) of each phase were combined in a test tube, followed by an aliquot (10-30 µL) of ^{111}In solution. The system was shaken mechanically (VWR Signature Digital Vortex Mixer) at 3000 rpm for 5 min and then centrifuged (Eppendorf model 5702) at 4400 rpm for 1 min. An aliquot (usually 250 µL) of each phase was measured with a NaI detector (Hidex AMG Model 425-601 and PerkinElmer Wizard 2480 automated gamma counters). The distribution ratio (D) and extraction efficiency (E) values were calculated as

$$D = \frac{I_{org}}{I_{aq}} \cdot \frac{V_{aq} \cdot \rho_{org}}{m_{org}} \quad \text{Eq. 1}$$

$$E = \frac{D}{1+D} \cdot 100\ \% \quad \text{Eq. 2}$$

where I_{org}, I_{aq} are decay-corrected net count rates of the measured nuclide per V_{aq} volume of aqueous phases and m_{org} and ρ_{org} are masses and densities of organic phases, respectively.

Results and Discussion

The starting materials for the binary mixtures in this study have been prescreened to have a low toxicity, a melting point below 100˚C and be commercially available. The melting temperature, enthalpy of fusion, and glass transition temperature of the pure chosen compounds can be found in Table 2 (thermograms are included in the ESI, Fig. S1). The measured values display a slight downward deviation from those in the literature. This deviation is attributed to the presence of minor impurities that may cause a melting point depression.

Of the five selected compounds, three are common pharmaceuticals. Lidocaine and ibuprofen are used for local anesthesia[67] and anti-inflammatory medicinal purposes,[68] respectively. Menthol is an extractant of peppermint oil[69] found in cigarettes to reduce throat inflammation,[40] as well as improve drug solubility and therefore promote membrane transport of both lidocaine[63] and ibuprofen.[70,71] Methyl anthranilate is a U.S. Federal Drug Administration (FDA) approved compound found in both sunscreen[72] and beverages,[73] earning the common name “grape smell” for its distinct aroma. Lastly, 1,8-Bis(dimethylamino)naphthalene belongs to a class of strongly basic ternary diamines called Proton Sponge®. These diamines have been used as catalysts in organic synthesis, such as in the conversion of carboxylic acids to isocyanates.[74] As one of the strongest known organic bases, Proton Sponge® forms mixtures of particular interest of this study. Moreover, it demonstrates a strong coordination ability to transition metals.[75] The structure of each compound and corresponding pK_a values can be found in Table 1.

Characterization of Binary Mixtures

Prediction of Homogeneous Liquids. Based on the principle of ideal solubility,[76] the mole fraction (x) of a saturated solution at temperature T can be predicted by the thermal properties of the pure compounds, such that:

$$ln x_1^{ideal} = \frac{\Delta h_m^{fus}}{R} \cdot \left(\frac{1}{T_m} - \frac{1}{T}\right) - \frac{1}{RT}\int_{T_m}^{T} \Delta c_p dT + \frac{1}{R}\int_{T_m}^{T} \frac{\Delta c_p}{T} dT \quad \text{Eq. 3}$$

where Δh_m^{fus}, Δc_p, and T_m refer to the enthalpy of fusion (kJ/mol), differential heat capacity (kJ/mol-K), and melting temperature (K) of the pure compound, respectively. To a first order approximation, the differential heat capacity can be assumed to be zero, resulting in simplifying Eq. 3 by eliminating the last two terms.[76] This simplified version has previously been applied to eutectics to describe the solubility and phase behavior of binary systems.[77]

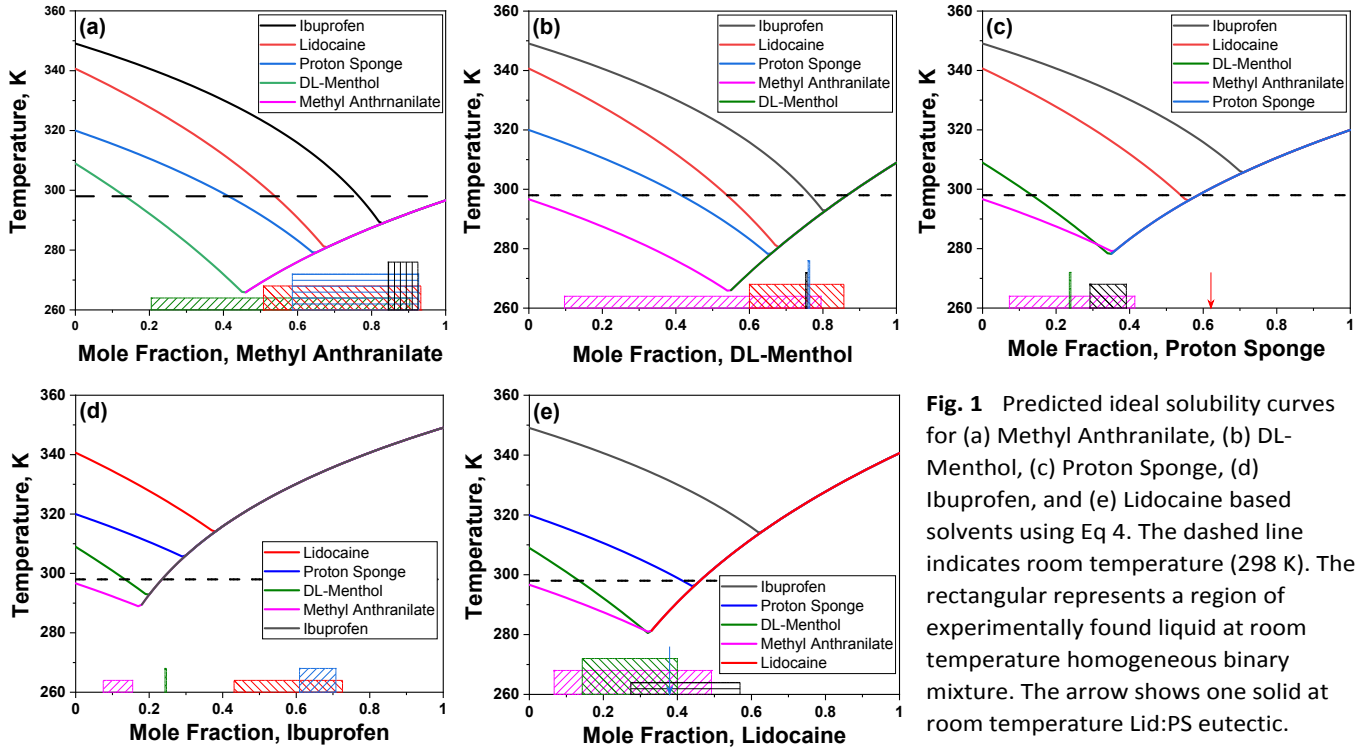

Fig. 1 Predicted ideal solubility curves for (a) Methyl Anthranilate, (b) DL-Menthol, (c) Proton Sponge, (d) Ibuprofen, and (e) Lidocaine based solvents using Eq 4. The dashed line indicates room temperature (298 K). The rectangular represents a region of experimentally found liquid at room temperature homogeneous binary mixture. The arrow shows one solid at room temperature Lid:PS eutectic.

Furthermore, assuming that the differential heat capacity of the pure compounds is equal to the molar entropy of fusion at the triple point, the equation simplifies to

$$lnx_1^{ideal} = -\frac{\Delta h_m^{fus}}{RT_m} ln\frac{T_m}{T} \quad \text{Eq. 4}$$

This adjustments has been shown to better fit experimental data and as a result is commonly used for pharmaceuticals.[78] Using Eq. 4 and the measured enthalpy and melting temperature of the pure compounds, the ideal phase behavior for the binary systems in this study has been predicted (Fig. 1). The predicted solubility curves of the binary systems displays a depression in melting temperature, which results in the formation of a eutectic where this depression is at a maximum (the lowest temperature).

The analysis of Fig. 1 shows that not every binary system considered will form a liquid at room temperature mixture. In particular, Ibu:PS, Ibu:Lid, and Lid:PS ideal mixtures are predicted to be solid at room temperature. However, only one of these mixtures (Lid:PS) forms room temperature solids across the entire mole ratio range. Given that the other two systems form room temperature liquids, there is a clear negative deviation in the phase transition temperature from ideality. Interestingly, Eq. 4 not only predicts Ibu:PS and Ibu:Lid to be solid, but the predicted eutectic composition is not in the range of room temperature liquids. Most likely this is the result of strong hydrogen bonding between the base (Lid and PS) and ibuprofen, a carboxylic acid. The model does take into account chemical interactions between the compounds, which have been shown to influence phase behavior.[11] In the thermograms of both Ibu:PS and Ibu:Lid, the lack of a melting peak indicated that these are LTTM's. In the both menthol- and methyl anthranilate-based systems, the predicted range of room temperature liquids matches well with the observed composition of liquids, indicating that Eq. 4 is a suitable model to describe the phase behavior of these mixtures, even though no melting peak is observed. Given that the phase behavior of the Mnt:Lid system has been previously studied, we only investigated the eutectic composition of 7:3.[71] Since the Lid:PS system forms only solids at room temperature (no deviation from ideality), this system is not suitable for LLE and won't be studied further in this work. All other binaries form liquid mixtures, however the Lid:Ibu system is also inconvenient for LLE due to very high viscosity observed (Temperature dependent viscosities are reported in Fig. S4). Physicochemical properties of selected binary mixtures with the lowest melting/glass transition temperatures are given in Table 3. It is important to note that the Ibu:PS liquid mixture unexpectedly demonstrates complete water miscibility despite that it was formed by water immiscible compounds. As a result, this particular low viscosity binary LTTM was also excluded from LLE experiments. As a primary screening, only mixtures that form hydrophobic homogenous low viscosity liquids at room temperature were selected due to their potential for solvent extraction.

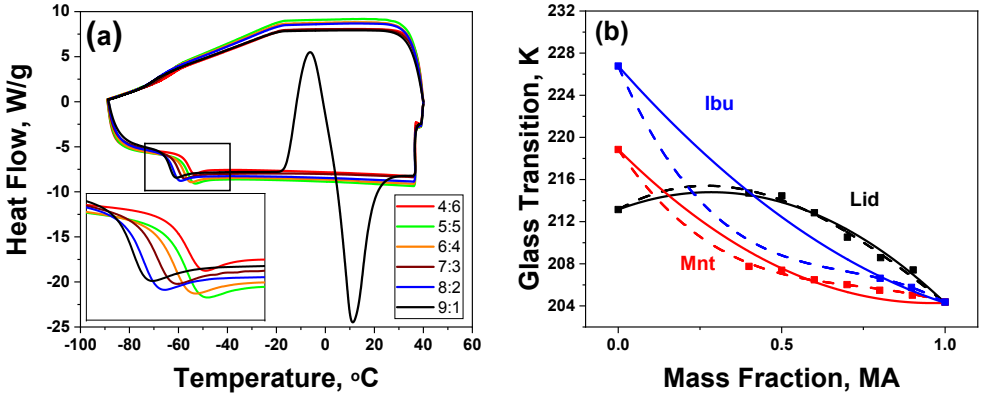

Fig. 2 DSC data for methyl anthranilate-based binary systems: (a) Thermograms of the methyl anthranilate-lidocaine liquid mixtures, reported as MA:Lid (w:w). The glass transition has been magnified; (b) Plot of the glass transition temperature as a function of mass composition, according to Eqs. 5 (solid lines) and 7 (dashed lines).

Intermolecular Hydrogen Bonding. The homogenous mixtures with liquidous room temperature LTTM were found to have no melting points, but rather have a glass transition temperature. For example, the thermograms of the liquidous methyl anthranilate – lidocaine system (from 100 to 40 wt% methyl anthranilate) display a glass transition around –70 to –50 ˚C (Fig. 2a, other systems reported in Fig. S2). The presence of a single endotherm (melting peak, glass transition, recrystallization, etc.) indicates complete thermodynamic miscibility between the two compounds.[62] When no clear melting behavior was observed, the composition corresponding to the LTTM was selected. The variation in glass temperature in the set of each liquidous binary mixture is dependent on the mass composition (Fig. 2b and Fig. S3). In order to study the nature of this dependency, two models have been adapted. Kwei[79] shows (eq. 5) that in polymers, the glass transition temperature can be given by modifying the Gordon-Taylor equation to describe the effect of hydrogen bonding between components in a mixture:

$$T_g = \frac{x_1 T_{g,1} + k(1-x_1)T_{g,2}}{x_1 + k(1-x_1)} + q x_1 (1-x_1); \quad \text{Eq. 5}$$

$$k = \frac{\rho_1 T_{g,1}}{\rho_2 T_{g,2}} \quad \text{Eq. 6}$$

where T_g, x, and ρ are the glass transition temperature, mass fraction, and density. The index 1 refers to the lower transition temperature of the two pure compounds. Kwei suggests that the fitting parameter q is proportional to the number of interactions as a result of all hydrogen bonding in the mixture. In the context of these binary solvents, a negative value of q indicates that the hydrogen bonding between the components in the mixture is weaker than the self-associative hydrogen bonding of the pure compounds. This model can be used to describe the weak interactions that promote liquid phase behavior in the organic phase. For example, ibuprofen contains a carboxylic group, a strong hydrogen bond donor. The q-values for ibuprofen-based systems increase (Ibu:Mnt < Ibu:MA < Ibu:Lid) with an increase of the second compound's pK_a (Table 4). This trend supports the hypothesis that the degree of hydrogen bonding can be attributed to the acidity of the pure compounds, and demonstrates the applicability of the Kwei function to non-polymer based systems.

Under the Kwei model, the deviation in glass transition temperature from the Gordon-Taylor model is attributed

Table 3 Physicochemical properties of selected water pre-saturated binary mixtures with minimal glass transition or melting temperature

Composition	Weight ratio	Temperature[a], °C	Dynamic Viscosity at 25.0 °C (cP)	Water Content (wt%)		Density (g/mL)
				Dry	Water Pre-Saturated	
MA:Lid	9:1	–61.17	10.880 ± 0.010	0.31 ± 0.03	1.6 ± 0.4	1.11
MA:Ibu	9:1	–63.09	10.85 ± 0.04	0.272 ± 0.017	1.65 ± 0.08	1.12
MA:PS	9:1	–63.21	9.43 ± 0.04	0.224 ± 0.016	0.98 ± 0.09	1.12
MA:Mnt	9:1	–64.93	8.350 ± 0.022	0.402 ± 0.013	1.50 ± 0.14	1.11
Mnt:Lid	5:5	–54.71	38.68 ± 0.04	0.174 ± 0.008	2.60 ± 0.14	0.90
Mnt:Ibu	7:3	–52.60	–	0.147 ± 0.008	1.96 ± 0.08	0.94
Mnt:PS	7:3	13.27 (M)	24.963 ± 0.021	0.072 ± 0.002	0.81 ± 0.20	0.88
Lid:Ibu	5:5	–26.26	790.8 ± 0.4	–	–	–
Ibu:PS[b]	6:4	–27.67	13,790 ± 7	–	–	–
Lid:PS[c]	4:6	30.42 (M)	–	–	–	–

[a] Glass transition unless noted as melting (M)
[b] Hydrophilic
[c] All mixtures are solid at room temperature

Table 4 Characterization of hydrogen bonding in binary mixtures

Mixture	Q	K_1	K_2
MA:Lid	19.5 ± 1.0	–3.0 ± 0.4	–1.2 ± 0.7
MA:Ibu	–12.8 ± 1.1	2.1 ± 0.1	1.8 ± 0.1
MA:Mnt	–19.0 ± 1.4	2.2 ± 0.1	1.8 ± 0.2
Mnt:Lid	–8.3 ± 1.4	0.3 ± 0.9	–2.9 ± 2.3
Mnt:Ibu	–58.4 ± 1.0	4.6 ± 0.1	–4.2 ± 0.1
Lid:Ibu	106 ± 5	–11.5 ± 0.6	–9.1 ± 1.4

solely to weak interactions, predominantly hydrogen bonding. More complex models exist that take into account additional parameters that affect the glass transition behavior. For example, Cui and Frank[62] summarize the power model adaptation to the Gordon-Taylor equation, taking into account the roll of conformational entropy in the system:

$$\frac{T_g - T_{g,2}}{T_{g,1} - T_{g,2}} = (1 + K_1)w_1 - (K_1 + K_2)w_1^2 + K_2 w_1^3 \qquad \text{Eq. 7}$$

The fitting parameter K_1 relates to the difference in interaction energies between the pure compounds and the binary mixtures, whereas K_2 is related to the conformational entropy change in the binary phase formation.[80] The calculated fitting parameters are summarized for both models in Table 4. As previously discussed, the phase behavior of these binary solvents is largely attributed to the formation of weak interactions between the two compounds. Therefore, the first order approximation in the Kwei model is suitable to describe the overall trends in hydrogen bonding in the solvents used in this study. For both models, the predicted glass transition temperature behavior of the binary system is dependent on those of the pure compounds. Proton Sponge® does not have an observed glass transition temperature, and therefore binary systems containing this compound could not be fit.

Aqueous Solubility. The solubility of a given organic compound has been shown to depend heavily both on its pK_a and the equilibrium pH.[81,82] Therefore, the equilibrium pH of aqueous phases after thorough mixing with each organic phase is reported in Fig. 3. We decided to focus on ternary amine based systems (i.e. Mnt:Lid, Mnt:PS, MA:Lid and MA:PS) as these systems were experimentally determined to be the most promising for indium extraction (discussed later).

When the observed equilibrium pH value is much lower than the pK_a of an organic compound, that compound can be assumed to exist predominantly in its neutral form (no protonation occurs). For example, the lowest observed pH values for the menthol-lidocaine and menthol-proton sponge systems are approximately 0.5 and 0.3, respectively. Given that menthol has a pK_a of –0.81 (Table 1), its full solubility can be written as

$$Mnt_{org} \overset{K_{sp}}{\leftrightarrow} Mnt_{aq} \qquad \text{Reaction 1}$$

with the corresponding solubility product of

$$K_{sp} = \frac{[Mnt]_{aq}}{[Mnt]_{org}} \qquad \text{Eq. 8}$$

When the pKa of a compound is near or above (i.e. relatively basic) the range of equilibrium pH values, the influence of protonation on solubility must be taken into account. This is because a charged organic species has a much greater hydrophilicity than its corresponding neutral form.[81,82] Both lidocaine and proton sponge are basic with high pK_a values (see Table 1), and therefore the protonation of each compound heavily influence their aqueous solubility. The transfer of either base, noted generally here as HBA for hydrogen bond acceptor, to the aqueous phase is given by

$$HBA_{org} \overset{K_{sp}}{\leftrightarrow} HBA_{aq} \qquad \text{Reaction 2}$$

$$HBA_{aq} + H^+{}_{aq} \overset{K_{pt}}{\leftrightarrow} HBA - H^+{}_{aq} \qquad \text{Reaction 3}$$

where the protonation constant K_{pt} is related to the K_a of the base by

$$K_{pt} = \frac{1}{K_a} \qquad \text{Eq. 9}$$

The overall solubility reaction can therefore be given as

$$HBA_{org} + H^+{}_{aq} \overset{K_{net}}{\leftrightarrow} HBA - H^+{}_{aq} \qquad \text{Reaction 4}$$

with the corresponding constant of

$$K_{net} = \frac{K_{sp}}{K_a} = \frac{[HBA - H^+]_{aq}}{[HBA]_{org}[H^+]_{aq}} \qquad \text{Eq. 10}$$

Given that the total mass of the base between the two phases is constant, the concentration of the base in the organic phase can be expressed as

$$[HBA]_{org,\,eq} = \frac{[HBA]_{org,int} \cdot V_{org,int} - [HBA]_{aq,\,eq} \cdot V_{aq,\,eq}}{V_{org,eq}} \qquad \text{Eq. 11}$$

where V denotes the volume of each phase and the initial volume and concentration of the organic phase are known. Based on the observed equilibrium pH values, it can be assumed that both lidocaine and proton sponge are almost completely protonated in the aqueous phase.

Therefore, Eq. 11 can be substituted into Eq. 10 to describe the overall pH-dependent solubility of the hydrogen bond donor as

$$[HBA]_{aq} \approx \frac{[HBA]_{int} \cdot V_{org,int} \cdot K_{net} \cdot [H^+]_{aq}}{V_{org} + V_{aq} \cdot K_{net} \cdot [H^+]_{aq}} \qquad \text{Eq. 12}$$

Fig. 4 reports the aqueous solubility of the corresponding hydrogen bond acceptor as a function of equilibrium pH. The lines are fit results according to Eq. 12. At low initial acid concentrations (corresponding to a high equilibrium pH) HBA is present in both the neutral (organic phase) and protonated (aqueous) forms (Reaction 4.) As the initial acid concentration increases (up to about pH 4-6), the solubility equilibrium is driven to the right and the $[HBA]_{aq}$ increases. Once the acid concentration is sufficient to convert all the base to its salt form, the compound exists only in the aqueous phase and the solubility curve plateaus. In the case of methyl anthranilate based systems, the equilibrium pH is low enough for protonation of methyl anthranilate above 1 M HCl. As this

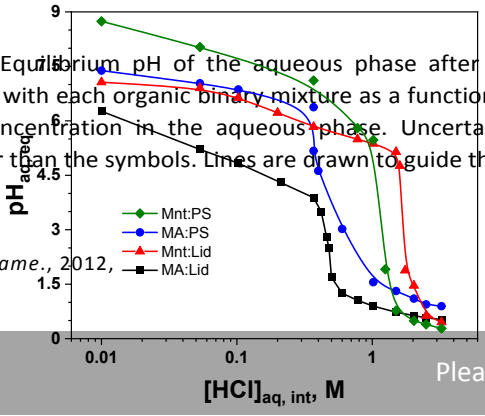

Fig. 3 Equilibrium pH of the aqueous phase after thorough mixing with each organic binary mixture as a function of initial HCl concentration in the aqueous phase. Uncertainties are smaller than the symbols. Lines are drawn to guide the eye.

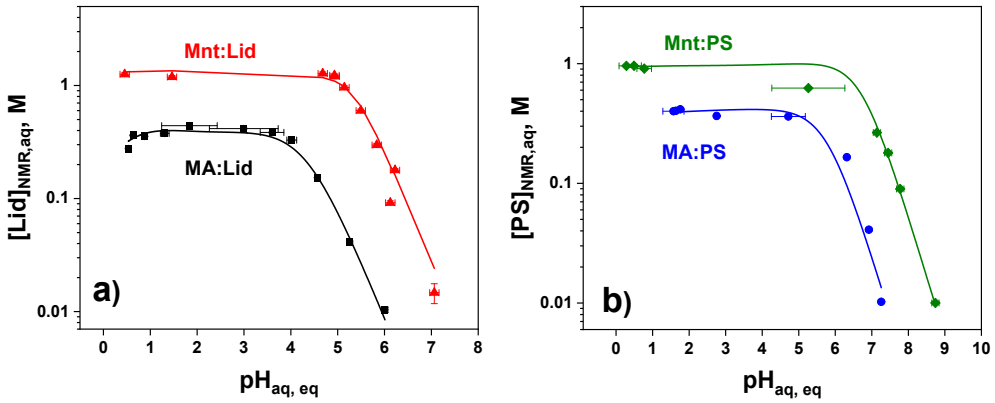

Fig. 4 pH-dependent aqueous phase solubility of the hydrogen bond acceptor for (a) lidocaine- and (b) proton sponge-based mixtures into hydrochloric acid. The subscript NMR indicates the total measured concentration (protonated and neutral combined). Lines are fit according to Eq. 12.

second compound moves to the aqueous phase it increases the total aqueous volume and dilutes the organic base. As a result, the measured concentration of the base decreases at a higher equilibrium pH (pH > 2.1). In the case of menthol based mixtures, the pK_a of menthol is much lower than the equilibrium pH, resulting in a relatively low aqueous concentration (< 20 mM) across the whole range of acid concentrations studied (Fig. S5). Therefore, the migration of menthol to the aqueous phase does not result in significant dilution of the HBA salt. By fitting the acid-dependent solubility data with Eq 12, the solubility constant K_{sp} can be calculated. It has been previously shown that menthol improved the solubility of lidocaine[63] and ibuprofen.[70] A similar trend is observed in this work, where the solubility constant for lidocaine along with menthol is $(1.6 \pm 0.3)\cdot 10^{-3}$, as compared to $(2.1 \pm 0.5)\cdot 10^{-4}$ for lidocaine along with methyl anthranilate. Analogous behavior is demonstrated in proton sponge-based mixtures, where dissolving the base and menthol yields a solubility product of $(3.6 \pm 0.4)\cdot 10^{-6}$. By contrast, proton sponge and methyl anthranilate has a product of $(4.1 \pm 0.7)\cdot 10^{-7}$. While it is observed that menthol increases the solubility product of the base by approximately an order of magnitude in both systems, the concentration of the neutral acceptor (Lid or PS) in the aqueous phase is much lower than the protonated form. Therefore, protonation and conversion of the acceptor to the hydrophilic salt is likely the main determinant of aqueous solubility.

Indium Behavior

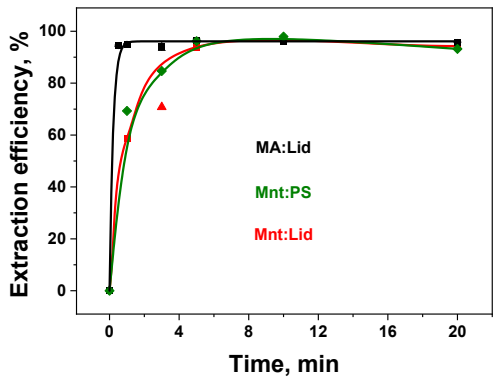

Fig. 5 Indium extraction from 0.05 M HCl into hydrophobic binary organic mixtures as a function of mixing time. Lines are drawn to guide the eye.

Kinetics of Indium Extraction. In order to systematically measure the behavior of indium in each solvent, a kinetic study must be carried out. After an initial screening to determine which binary mixtures demonstrate a capacity to extract indium, the distribution ratio of indium between each mixture and 0.05 M HCl was measures at various reaction times (Fig. 5). All systems appear to reach equilibrium conditions within 5 minutes of vigorous mixing. To maintain consistency and ensure equilibrium has been reached, 5 minute shaking is used for all reported results. As demonstrated in Fig. 5, the extraction of indium into menthol-based mixtures is slower than that of methyl anthranilate-based systems. This is likely the result of differences in the dynamic viscosity, where menthol-based mixtures have greater viscosities and therefore are not as easily mixed with aqueous systems (see Table 3).

Mechanism of Extraction. While ten sets of binary systems can be prepared from the 5 compounds listed in this work, three mixtures are not considered based on their physical characteristics. Lid:PS forms only solids at room temperature, Ibu:PS mixtures are hydrophilic, and Ibu:Lid forms solvents with too great of a viscosity to be suitable for solvent extraction (Table 3). The extraction of indium from 0.05 M HCl into the remaining 7 systems is reported in Table 5. Of these, 4 systems (MA:Lid, Mnt:Lid, MA:PS and Mnt:PS) demonstrate a capacity to extract indium with distribution ratios ranging from 2 to nearly 800 in 0.05 M HCl. For context, we have previously reported[41] indium extraction at the same acidity from binary

Table 5 Distribution ratio values for Indium extraction from 0.05 M HCl into binary systems. Uncertainties are calculated from the standard deviation of triplicate measurements

Mixture	Weight ratio	Water content dependency	
		Dry	Water pre-saturated
Mnt:Lid	5:5	2.14 ± 0.17	5.1 ± 0.9
Mnt:PS	7:3	4.1 ± 0.5	29.5 ± 0.5
MA:Lid	9:1	28 ± 5	5.49 ± 0.33
MA:PS	9:1	767 ± 27	270 ± 40
MA:Ibu	9:1	$(1.34 \pm 0.14)\cdot 10^{-3}$	$(1.19 \pm 0.06)\cdot 10^{-3}$
Mnt:Ibu	7:3	$(2.0 \pm 0.7)\cdot 10^{-4}$	$(1.63 \pm 0.14)\cdot 10^{-4}$
MA:Mn	9:1	$(5.9 \pm 1.3)\cdot 10^{-5}$	$(3.5 \pm 0.4)\cdot 10^{-5}$

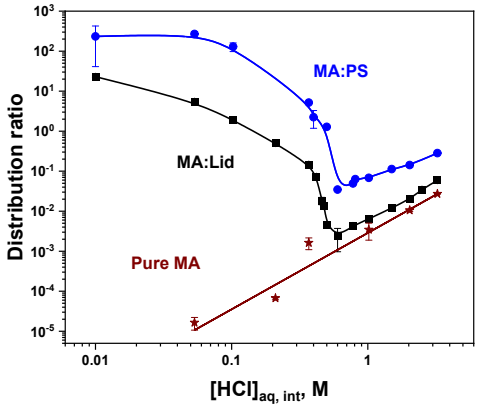

Fig. 6 Effect of initial acid concentration on the extraction of indium into water pre-saturated methyl anthranilate, MA:Lid and MA:PS. Lines are drawn to guide the eye.

mixtures of alkyl ammonium salts and carboxylic acids. These systems also demonstrate distribution ratios above 1 at 0.05 M HCl, though these mixtures have significantly different acid-dependent indium extraction behaviors due to differences in extraction mechanisms. Similarly, the extraction of indium from 0.05 M HCl into Mnt:Ibu (this work) and Mnt:Lauric acid[41] is nearly identical with $D \approx 2 \cdot 10^{-4}$. However, given that indium extraction into Mnt:Ibu, MA:Mnt and MA:Ibu is low ($D_{In} < 0.01$), these systems are not studied further in this work. Herein, all reported extraction values are measured from water pre-saturated systems to minimize the influence of physical effects.

In order to study the mechanism and scope of indium extraction, the initial HCl concentration is varied from 0.01 M to 3 M (Fig. 6). The MA:Lid system has been selected for study due to its relatively low viscosity and convenient indium D values among ternary amine based systems. To identify the chemical influence of each organic compound, the extraction of indium into pure methyl anthranilate and MA:PS was measured at the same HCl concentrations and added to Fig. 6.

The extraction of indium into MA:Lid appears to be strongly correlated to the aqueous solubility of the binary system. At low acidities, lidocaine is present in both phases and acts as buffer, neutralizing excess HCl and forming the aqueous LidHCl salt. When a sufficient amount of acid is present to protonate all of the lidocaine in the system, the equilibrium pH sharply decreases (Fig. 3). This drop in pH occurs at the same HCl concentration (~0.4 M) as a drastic decrease in the distribution ratio of indium (Fig. 6). One possible explanation for this behavior comes from the speciation of indium. It has been previously shown[83] that hydrolysis of indium chloride species occurs at pH >> 3. With a strong organic base present (lidocaine), neutral indium hydroxide and hydroxy chloride species could form and migrate to the organic phase, given by

$$InCl_n^{3-n}{}_{aq} + (3-n) \cdot H_2O_{aq} \rightleftarrows InCl_n(OH)_{3-n}{}_{org} + (3-n) \cdot H^+{}_{aq} \quad \text{Reaction 5}$$

As shown by the expression above, lidocaine plays an indirect role in indium extraction, consuming aqueous protons and driving the reaction equilibrium to the right. Such a phenomena also explains why MA:PS extracts more indium in this region, as PS is more basic and therefore consumes more protons. Furthermore, the extraction of indium into to pure methyl anthranilate is very low below 0.5 M HCl, suggesting that lidocaine is predominantly responsible for extraction at low acidities.

At higher initial acid concentrations, the system is too acidic to support indium hydrolysis. Therefore, a new mechanism is likely responsible for extraction in this range. The pure organic liquid (MA) demonstrates nearly the same extraction behavior as MA-Lid above 0.5 M HCl, indicating that methyl anthranilate is responsible for extraction in this acidity region. It has been previously shown that methyl anthranilate can act as a ligand for transition metals such as zinc[84] and copper.[85] We hypothesize that extraction is carried out through the formation of a metal-organic complex between neutral indium chloride and methyl anthranilate, given by

$$a \cdot C_8H_9NO_{2aq} + InCl_{3aq} \rightleftarrows (C_8H_9NO_2)_a InCl_{3org} \quad \text{Reaction 6}$$

Indium is known to have a coordinating number of 6. With 3 chlorides present in the extracted species, a maximum of 3 molecules could coordinate in the extracted complex. Given that this complex forms in the aqueous phase, it would be hydrated with 1 or 2 molecules of water when *a* is 2 or 1, respectively.

The mechanism of extraction proposed in reactions 5 and 6 can be used to mathematically fit the experimental distribution ratio of indium in order to determine the contribution of each indium species to the total amount of indium extracted. The distribution ratio is defined as

$$D_{in} = \frac{\sum[In]_{org}}{\sum[In]_{aq}} \quad \text{Eq. 13}$$

where the sum of the organic indium species depends on the mechanism of extraction and the aqueous sum is determined by known speciation.[83] Based on the proposed mechanism of extraction, this expression can be expanded as

$$D_{In} = \frac{\sum[In]_{org}}{\sum[In]_{aq}} = \frac{\sum[InCl_n(OH)_{3-n}]_{org} + [(C_8H_9NO_2)_a InCl_3]_{org}}{\sum[In]_{aq}} \quad \text{Eq. 14}$$

Relation between different aqueous indium species can be described generally as

$$In^{3+} + nCl^- + mH_2O \rightleftarrows InCl_n(OH)_m{}^{3-n-m} + mH^+ \quad \text{Reaction 7}$$

The stability constants for $m = 0$, namely pure indium chloride species, have been reported by Sato.[86] The cumulative stability constant β is used to describe these species and is defined as

$$\beta_n = \frac{[InCl_n^{3-n}]}{[In^{3+}][Cl^-]^n}, \; 1 \le n \le 6 \quad \text{Eq. 15}$$

While 6 coordinating chlorides are possible, the studied range of HCl concentrations is not high enough to support the formation of the penta and hexachloride indium anions.[83,86] In the case of indium hydroxide and mixed hydroxy chloride species, the stability constants used in this work are reported by Mesmer.[83] Similarly, these stability constants are defined as

$$\Upsilon_{n,m} = \frac{[InCl_n(OH)_m{}^{3-n-m}][H^+]^m}{[In^{3+}][Cl^-]^n}, \quad 0 \le n \le 2, 1 \le m \le 3, n+m \le 3 \quad \text{Eq. 16}$$

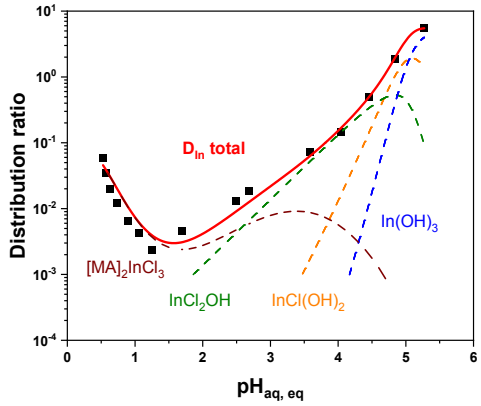

Fig. 7 Extraction of indium from HCl into MA:Lid (wet) as a function of equilibrium aqueous pH. The lines are fit according to eq. 21, with the solid line showing the complete fit and the dashed lines indicating the contribution of each individual species, calculated by setting all other extraction constants to zero. Uncertainties are smaller than the symbol size.

The total indium concentration in the aqueous phase is given by

$$\sum[In]_{aq} = [In^{3+}] + \sum_{n=1}^{4}\beta_n[In^{3+}][Cl^-]^n + \sum_{m=1}^{3}\frac{Y_m[In^{3+}]}{[H^+]^m} + \sum_{m,n=1}^{n+m\leq 3}\frac{[In^{3+}][Cl^-]^n}{[H^+]^m} \quad \text{Eq. 17}$$

The concentration of organic indium species will be determined by the proposed mechanism of extraction. In the case of high pH extraction predicted by Reaction 5, the concentration of the extracted species is given by rearranging the expression for the equilibrium constant to yield

$$InCl_n(OH)_{3-n\,org} = \frac{K_{ext}\cdot[InCl_n^{3-n}]_{aq}}{[H^+]^{3-n}} \quad \text{Eq. 18}$$

The stability constant of indium chloride can be substituted into this expression, giving

$$InCl_n(OH)_{3-n\,org} = \frac{K_{ext}\cdot\beta_n\cdot[In^{3+}]\cdot[Cl^-]^n}{[H^+]^{3-n}} \quad \text{Eq. 19}$$

At higher acid concentrations, a similar prediction made for the proposed metal organic complex (Reaction 6)

$$(C_8H_9NO_2)_aInCl_{3\,org} = K'_{ext}\cdot\beta_3\cdot[C_8H_9NO_2]_{aq}{}^a\cdot[In^{3+}]\cdot[Cl^-]^3 \quad \text{Eq. 20}$$

Combining terms for both the aqueous and organic indium concentrations, the expression for the total distribution ratio becomes

$$D_{In} = \frac{\sum[In]_{org}}{\sum[In]_{aq}} = \frac{\sum K_{ext_n}\cdot\beta_n\cdot[Cl^-]^n\cdot[H^+]^{-(3-n)} + K'_{ext}\cdot\beta_3\cdot[C_8H_9NO_2]_{aq}{}^a[Cl^-]^3}{1+\sum_{n=1}^{4}\beta_n[Cl^-]^n + \sum_{m=1}^{3}\frac{Y_m}{[H^+]^m} + \sum_{m,n=1}^{n+m\leq 3}Y_{n,m}\frac{[Cl^-]^n}{[H^+]^m}} \quad \text{Eq. 21}$$

Importantly, the concentration of bare indium [In^{3+}] cancels out, yielding an expression for the distribution ratio of indium that depends only on the known set of stability constants β and Y, the equilibrium chloride and proton concentrations, and the constants of extraction K_{ext} and K'_{ext}. These extraction constants can be calculated through applying equation 21 to the pH-dependent data of indium extraction into MA-Lid (Fig. 7). Through fitting this data set, 3 neutral OH-based indium complexes are predicted to be extracted as described in reaction 5. The calculated equilibrium constants (K_{ext}) are (2.04 ± 0.02) · 10^{-12}, (1.28 ± 0.03) · 10^{-9}, and (1.53 ± 0.05) · 10^{-5} for $In(OH)_3$, $InCl(OH)_2$, and $InCl_2OH$, respectively. In the lower pH range, a single complex consisting of 2 molecules of methyl anthranilate and $InCl_3$ is proposed as the predominant extracted species (Reaction 6, a = 2), with a constant of extraction (K'_{ext}) of (8 ± 1) · 10^2.

To determine the contribution of each extracted species to the total distribution ratio of In (solid line in Fig. 7), the calculated constants of extraction were substituted individually into eq. 21 with the other 3 constants fixed at zero. These substitutions yield four theoretical models corresponding to the four extracted species (dashed lines in Fig. 7). An analysis of Fig. 7 reveals that between pH 2.5 and 5.5, an increase in the number of OH^- ions coordinating to indium leads to higher overall extraction. This behavior can be rationalized by the high aqueous solubility of indium chloride[87] (1.95 g/mL) and near complete insolubility of indium hydroxide in water. As a result, a higher number of ligating hydroxides could produce a more hydrophobic (and therefore more extractable) complexes. To summarize, the mathematical model developed in this work predicts the extraction of neutral indium species of the form $InCl_n(OH)_{3-n}$ when pH_{eq} > 2. The inclusion of a basic hydrogen bond donor such as lidocaine or Proton Sponge® promotes extraction indirectly by consuming aqueous protons, thus altering the speciation of indium. When pH_{eq} < 2, MA is proposed to play a direct role in extraction by forming a bulky neutral species $[MA]_2InCl_3$ that migrates to the organic phase. Thus we establish a method for describing the role of speciation and solubility in indium extraction from HCl into hydrophobic binary mixtures.

Conclusions

The applications of hydrophobic binary mixtures of menthol, lidocaine, proton sponge®, ibuprofen, and methyl anthranilate for indium extraction have been investigated. The composition of homogeneous room temperature liquids was found to be well predicted by classical principles of ideal solubility, establishing an effective screening technique for the development of similar solvents. Additionally, composition dependent glass transition temperature of these binary systems is demonstrated to be a useful indication of the extent of hydrogen bonding networks that form on each binary system. We show that lidocaine and proton sponge® display remarkable extracting properties when coupled with a suitable hydrogen bond donor. Lastly, a mathematical model is developed based on the mechanism of extraction to determine the contribution of each indium species to the total extraction of indium into the binary mixture. Based on the results reported in this work, neutral indium hydroxide and hydroxy chloride molecules are identified as the predominantly extracted species at low initial HCl concentrations. We also report on the role of methyl anthranilate in indium extraction when the concentration of HCl exceeds 0.5 M. These findings provide a framework for

studying sustainable, cost effective alternatives to conventional solvents and ionic liquids for metal extraction.

Conflicts of interest

There are no conflicts to declare.

Acknowledgements

This material is based upon work supported by the U.S. Department of Energy, Office of Science, Office of Nuclear Physics under Award Number DE-FG02-93ER40773, National Nuclear Security Administration through the Nuclear Science and Security Consortium under Award Number DE-NA-0003180 and the National Science Foundation (PHY-1659847). This report was prepared as an account of work sponsored by an agency of the United States Government. Neither the United States Government nor any agency thereof, nor any of their employees, makes any warranty, express or implied, or assumes any legal liability or responsibility for the accuracy, completeness, or usefulness of any information, apparatus, product, or process disclosed, or represents that its use would not infringe privately owned rights. Reference herein to any specific commercial product, process, or service by trade name, trademark, manufacturer, or otherwise does not necessarily constitute or imply its endorsement, recommendation, or favoring by the United States Government or any agency thereof. The views and opinions of authors expressed herein do not necessarily state or reflect those of the United States Government or any agency thereof. Financial support from the National Center for Scientific Research (CNRS, France) through its International Program for Scientific Cooperation (PICS) is gratefully acknowledged.

References

1. S. Abou-Shehada, J. H. Clark, G. Paggiola and J. Sherwood, *Chem. Eng. Process.*, 2016, **99**, 88.
2. L. Ren, Q. Wu, C. Yang, L. Zhu, C. Li, P. Zhang, H. Zhang, X. Meng and F.-S. Xiao, *J. Am. Chem. Soc.*, 2012, **134**, 15173.
3. D. Constable, C. Jimenez-Gonzalez and R. K. Henderson, *Org. Process Res. Dev.*, 2007, **11**, 133.
4. F. M. Kerton and R. Marriott, *Alternative Solvents for Green Chemistry*, Royal Society of Chemistry, Cambridge, 2013.
5. C. Clarke, W.-C. Tu, O. Levers, A. Brohl and J. Hallett, *Chem. Rev.*, 2018, **118**, 747.
6. M. Armand, F. Endres, D. R. MacFarlane, H. Ohno and B. Scrosati, in *Materials for Sustainable Energy: A Collection of Peer-Reviewed Research and Review Articles from Nature Publishing Group*, World Scientific, London, 2011, pp. 129.
7. J. Huddleston, H. Willauer, R. Swatloski, A. Visser and R. Rogers, *Chem. Commun.*, 1998, 1765.
8. E. E. Tereshatov, M. Y. Boltoeva, V. Mazan, M. F. Volia and C. M. Folden III, *J. Phys. Chem. B.*, 2016, **120**, 2311.
9. T. Vander Hoogerstraete, S. Wellens, K. Verachtert and K. Binnemans, *Green Chem.*, 2013, **15**, 919.
10. S. Dutta and K. Nath, *J. Water Eng.* , 2018, **21**, 163.
11. M. Francisco, A. van den Bruinhorst and M. C. Kroon, *Angew. Chem. Int. Edit.*, 2013, **52**, 3074.
12. M. Francisco, A. van den Bruinhorst and M. C. Kroon, *Green Chem.*, 2012, **14**, 2153.
13. R. Stefanovic, M. Ludwig, G. Webber, R. Atkin and A. Page, *Phys. Chem. Chem. Phys.*, 2017, **19**, 3297.
14. M. Martins, S. Pinho and J. Coutinho, *J. Solution Chem.*, 2018, **48**, 962.
15. H. Wu, Z. Deng, B. Zhou, M. Qi, M. Hong and G. Ren, *J. Mol. Liq.*, 2019, **283**, 339.
16. E. L. Smith, A. P. Abbott and K. S. Ryder, *Chem. Rev.*, 2014, **114**, 11060.
17. H. Zhao and G. A. Baker, *J. Chem. Technol. Biot.*, 2013, **88**, 3.
18. C. Deferm, B. Onghena, V. Nguyen, D. Banerjee, J. Fransaer and K. Binnemans, *RSC Adv.*, 2020, **10**, 24595.
19. M. F. Volia, E. E. Tereshatov, M. Boltoeva and C. M. Folden III, *New J. Chem.*, 2020, **44**, 2527.
20. S. van Roosendael, M. Regadío, J. Roosen and K. Binnemans, *Sep. Purif. Technol.*, 2019, **212**, 843.
21. C. Deferm, J. Luyten, H. Oosterhof, J. Fransaer and K. Binnemans, *Green Chem.*, 2018, **20**, 412.
22. K. Cubova, M. Semelova, M. Nemec, J. John, J. Milacic, J. P. Omtvedt and J. Stursa, *J. Radioanal. Nucl. Chem.*, 2018, **318**, 2455.
23. M. Matsumiya, M. Sumi, Y. Uchino and I. Yanagi, *Sep. Purif. Technol.*, 2018, **201**, 25.
24. C. Deferm, B. Onghena, T. Vander Hoogerstraete, D. Banerjee, J. Luyten, H. Oosterhof, J. Fransaer and K. Binnemans, *Dalton T.*, 2017, **46**, 4412.
25. N. Schaeffer, S. M. Grimes and C. R. Cheeseman, *Inorg. Chim. Acta*, 2017, **457**, 53.
26. C. Deferm, M. Van de Voorde, J. Luyten, H. Oosterhof, J. Fransaer and K. Binnemans, *Green Chem.*, 2016, **18**, 4116.
27. E. E. Tereshatov, M. Y. Boltoeva and C. M. Folden, *Solvent Extr. Ion Exch.*, 2015, **33**, 607.
28. T. Vander Hoogerstraete, B. Onghena and K. Binnemans, *J. Phys. Chem. Lett.*, 2013, **4**, 1659.
29. S. Katsuta, M. Okai, Y. Yoshimoto and Y. Kudo, *Anal. Sci.*, 2012, **28**, 1009.
30. J. B. Ghasemi and E. Zolfonoun, *Environ. Monit. Assess.*, 2012, **184**, 3971.
31. F. Kubota, Y. Shimobori, Y. Koyanagi, K. Nakashima, K. Shimojo, N. Kamiya and M. Goto, *Solvent Extr. Res. Dev.*, 2009, **16**, 151.
32. A. Yoshimura, I. Daigo and Y. Matsuno, *Mater. Trans.*, 2013, **54**, 102.
33. E. McCullough and N. T. Nassar, *Mineral Econ.*, 2017, **30**, 257.
34. Report on Critical Raw Materials and the Circular Economy, https://publications.europa.eu/en/publication-detail/-/publication/d1be1b43-e18f-11e8-b690-01aa75ed71a1/language-en/format-PDF/source-80004733, 2020).
35. National Minerals Information Center, https://www.usgs.gov/centers/nmic).
36. C. Florindo, L. Branco and I. Marrucho, *Fluid Phase Equilibr.*, 2017, **448**, 135.
37. J. Cao, M. Yang, F. Cao, J. Wang and E. Su, *ACS Sustain. Chem. Eng.*, 2017, **5**, 3270.
38. D. van Osch, L. F. Zubeir, A. van den Bruinhorst, M. A. Rocha and M. C. Kroon, *Green Chem.*, 2015, **17**, 4518.
39. B. D. Ribeiro, C. Florindo, L. C. Iff, M. A. Coelho and I. M. Marrucho, *ACS Sustain. Chem. Eng.*, 2015, **3**, 2469.
40. G. F. Wayne and G. N. Connolly, *Nicotine Tob. Res.*, 2004, **6**, S43.
41. E. E. Tereshatov, M. Y. Boltoeva and C. M. Folden III, *Green Chem.*, 2016, **18**, 4616.

42. D. van Osch, D. Parmentier, C. H. Dietz, A. van den Bruinhorst, R. Tuinier and M. C. Kroon, *Chem. Commun.*, 2016, **52**, 11987.
43. N. Schaeffer, M. A. Martins, C. M. Neves, S. P. Pinho and J. A. Coutinho, *Chem. Commun.*, 2018, **54**, 8104.
44. T. Phelps, N. Bhawawet, S. Jurisson and G. Baker, *ACS Sustain. Chem. Eng.*, 2018, **6**, 13656.
45. N. Schaeffer, J. Conceição, M. Martins, M. Neves, G. Pérez-Sánchez, J. Gomes, N. Papaiconomou and J. Coutinho, *Green Chem.*, 2020, **22**, 2810.
46. M. Deetlefs and K. R. Seddon, *Green Chem.*, 2010, **12**, 17.
47. J. Huang, X. Guo, T. Xu, L. Fan, X. Zhou and S. Wu, *J. Chromatogr. A*, 2019, **1598**, 1.
48. A. P. Abbott, E. I. Ahmed, K. Prasad, I. B. Qader and K. Ryder, *Fluid Phase Equilibr.*, 2017, **448**, 2.
49. Menthol Product Sheet, https://www.drugbank.ca/drugs/DB00825).
50. S. Bitteur and R. Rosset, *Chromatographia*, 1989, **27**, 194.
51. A. C. Cumming, *P. R. Soc. A.*, 1906, **78**, 103.
52. R. Bushra and N. Aslam, *Oman Med. J.*, 2010, **25**, 155.
53. M. F. Powell, *Pharm. Res.*, 1987, **4**, 42.
54. V. Sanchez, G. R. Arthur and G. R. Strichartz, *Aneth. Analg.*, 1987, **66**, 159.
55. R. Alder, P. Bowman, W. Steele and D. Winterman, *Chem. Commun.*, 1968, **452**, 723.
56. T. Cordeiro, C. Castiñeira, D. Mendes, F. Danède, J. Sotomayor, I. M. Fonseca, M. Gomes da Silva, A. Paiva, S. Barreiros and M. M. Cardoso, *Mol. Pharm.*, 2017, **14**, 3164.
57. J. Chickos, D. Garin, M. Hitt and G. Schilling, *Tetrahedron*, 1981, **37**, 2255.
58. D. R. Lide, *CRC Handbook of Chemistry and Physics*, Boca Raton, Florida, 81 edn., 2000.
59. A. R. Paradkar, M. Maheshwari, A. R. Ketkar and B. Chauhan, *Int. J. Pharm.*, 2003, **255**, 33.
60. A. Nokhodchi, O. Amire and M. Jelvehgari, *Daru*, 2010, **18**, 74.
61. E. Dudognon, F. Danède, M. Descamps and N. T. Correia, *Pharm. Res.*, 2008, **25**, 2853.
62. Y. Cui and S. Frank, *J. Pharm. Sci.*, 2006, **95**, 701.
63. L. Kang, H. Jun and J. McCall, *Int. J. Pharm.*, 2000, **206**, 35.
64. M. Lazerges, I. B. Rietveld, Y. Corvis, R. Céolin and P. Espeau, *Thermochim. Acta*, 2010, **497**, 124.
65. Proton Sponge Safety Data Sheet https://www.sigmaaldrich.com/MSDS/MSDS/DisplayMSDSPage.do?country=US&language=en&productNumber=158496&brand=ALDRICH&PageToGoToURL=https%3A%2F%2Fwww.sigmaaldrich.com%2Fcatalog%2Fproduct%2Faldrich%2F158496%3Flang%3Den, (accessed June 14, 2020).
66. R. L. Benoit, D. Lefebvre and M. Fréchette, *Can. J. Chem.*, 1987, **65**, 996.
67. M. S. Gold, D. B. Reichling, K. F. Hampl, K. Drasner and J. D. Levine, *J. Pharmacol. Exp. Ther.*, 1998, **285**, 413.
68. M. Busson, *J. Int. Med. Res.*, 1986, **14**, 53.
69. A. Ammann, D. C. Hinz, R. S. Addleman, C. M. Wai and B. W. Wenclawiak, *Fresen. J. Anal. Chem.*, 1999, **364**, 650.
70. C. S. Yong, C. H. Yang, J.-D. Rhee, B.-J. Lee, D.-C. Kim, D.-D. Kim, C.-K. Kim, J.-S. Choi and H.-G. Choi, *Int. J. Pharm.*, 2004, **269**, 169.
71. P. W. Stott, A. C. Williams and B. W. Barry, *J. Controlled Release*, 1998, **50**, 297.
72. V. DeLeo, *Dermatol. Clin.*, 2006, **24**, 27.
73. R. Nelson, T. Acree, C. Lee and R. Butts, *J. Food Sci.*, 1977, **42**, 57.
74. J. W. Gilman and Y. A. Otonari, *Synthetic Commun.*, 1993, **23**, 335.
75. T. Yamasaki, N. Ozaki, Y. Saika, K. Ohta, K. Goboh, F. Nakamura, M. Hashimoto and S. Okeya, *Chem. Lett.*, 2004, **33**, 928.
76. H. Hojjati and S. Rohani, *Org. Process Res. Dev.*, 2006, **10**, 1101.
77. A. van den Bruinhorst, S. Raes, S. A. Maesara, M. C. Kroon, A. C. C. Esteves and J. Meuldijk, *Sep. Purif. Technol.*, 2019, **216**, 147.
78. S. H. Neau, S. V. Bhandarkar and E. W. Hellmuth, *Pharm. Res.*, 1997, **14**, 601.
79. T. Kwei, *J. Polym. Sci. Pol. Lett.*, 1984, **22**, 307.
80. T. Vilics, H. A. Schneider, V. Manoviciu and I. Manoviciu, *Polymer*, 1997, **38**, 1865.
81. G. Volgyi, E. Baka, K. J. Box, J. E. Comer and K. Takacs-Novak, *Anal. Chim. Acta.*, 2010, **673**, 40.
82. C. A. Bergstrom, K. Luthman and P. Artursson, *Eur. J. Pharm. Sci.*, 2004, **22**, 387.
83. R. Mesmer and C. Baes, in *The Hydrolysis of Cations*, John Wiley and Sons, 1976, pp. 319.
84. S. Boudreau and H. Haendler, *Acta Crystallogr. C*, 1992, **48**, 615.
85. S. Boudreau and H. Haendler, *Acta Crystallogr. C*, 1986, **42**, 980.
86. T. Sato, *Shigen-to-Sozai*, 1996, **112**, 123.
87. Indium Chloride Product Sheet, https://www.americanelements.com/indium-iii-chloride-10025-82-8, (accessed June 14, 2020).